Elasticity of the Oriented Mesomorphic Form of Syndiotactic Polypropylene

Liberata Guadagno, Concetta D'Aniello, Carlo Naddeo, and Vittoria Vittoria*

Dipartimento di Ingegneria Chimica e Alimentare, Università di Salerno, Via Ponte Don Melillo, 84084 Fisciano, Salerno, Italy

Stefano Valdo Meille

Dipartimento di Chimica, Materiali ed Ingegneria Chimica "G. Natta", Politecnico di Milano, Via Mancinelli 7, 20131 Milano, Italy

Received October 22, 2001; Revised Manuscript Received February 11, 2002

ABSTRACT: Syndiotactic polypropylene (sPP) was melt-quenched in an ice−water bath and directly drawn at 0 °C up to a draw ratio of 6. The oriented sample was kept in the cold bath for 10 days under tension, and then analyzed at room temperature either fixed or after releasing tension. The fully extended fiber showed by X-ray diffraction essentially the trans-planar crystalline form III. Upon relaxation, the sample transformed in high proportion to the trans-planar mesomorphic form, free of reflections of helical crystal forms, and became elastic. In this process, there is a reduction of both crystallinity and crystallite orientation. Since the crystalline and mesomorphic chain conformation is trans in both the stretched and relaxed fiber, the elastic behavior in the present sample does not involve a conformational transition in the crystalline domains. At variance, in the infrared spectrum of the relaxed but not of the stretched sample, one of the bands diagnostic of the helical conformation appears. Thus, when the fiber is unhooked, chains tend to disorder reversibly and some segments adopt the helical conformation, even if they must reside in the amorphous component connecting the more ordered mesomorphic domains. Reversible crystallization of the mesophase and of the partially oriented, intercrystalline, amorphous chains into highly oriented metastable trans-planar form III appears to be responsible for the elastic behavior of sPP fibers in the present study. Models of the structural organization in the trans-planar mesophase and the implications of our results with respect to the general mechanism leading to the elastic behavior of sPP are discussed.

Introduction

It is generally acknowledged that the macroscopic properties of polymeric materials are strongly influenced by the structural organization, which is in turn driven by physical treatments. In this respect, the behavior of syndiotactic polypropylene (sPP) is emblematic. This polymer, when cooled from the quiescent melt, is partially crystalline and behaves as a typical semicrystalline system. It can be stretched up to seven times the initial length, showing a high strain-hardening typical of a plastic deformation.[1−4] Nevertheless, as soon as the tension on the sample is released, the fiber shows an elastic behavior undergoing a large shrinkage.[5] The elasticity, closely correlated to the structural organization of the fibers, is not shown at all by original unoriented films, in whatever form—either helical or trans-planar—they were, demonstrating the profound influence of the morphology on the physical properties. However, the difficulty correlating the elastic behavior to the structural organization of sPP is principally due to its very complex polymorphism,[6−20] not yet fully understood.

Four crystalline forms of sPP have been described so far, characterized by 2-fold helical, trans-planar or $(T_6G_2T_2G_2)_n$ conformations in different crystalline cells. In forms I and II chains adopt $(T_2G_2)_n$ helical conformation,[6,14−16] whereas form III and IV present chains in trans-planar and $(T_6G_2T_2G_2)_n$ conformations,[10,11] respectively. Form I is the stable form of sPP obtained under the most common crystallization conditions both from the melt and from solution as single crystals.[6−9,15] In this form, right and left-handed helices alternate along both axes of the unit cell, which is orthorhombic with a = 14.50 Å, b = 11.20 Å, and c = 7.45 Å. Samples crystallized from the melt at low temperatures present disorder in this regular alternation with an orthorhombic lattice where a and c remain the same and b is halved.

Form II corresponds to a C-centered structure in which the helical chains share the same chirality. So far it was obtained stretching at room-temperature compression molded specimens of low stereoregularity.[16] The trans-planar form III is a metastable polymorph of sPP and also presents an orthorhombic lattice with a = 5.22 Å, b = 11.17 Å, and c = 5.05 Å. It is obtained by cold drawing of sPP samples, quenched from melt to low temperatures.[10] Recently the spontaneous crystallization of an unoriented trans-planar form was reported, also quenching sPP samples from the melt to a 0 °C bath and keeping the specimen at that temperature for a long time.[21−24] This novel form was interpreted either as the crystalline form III[21] or as a mesophase showing lateral disorder in the packing of the trans-planar chains.[22]

The complex polymorphic behavior of sPP, also dependent on the tacticity and the molecular weight of the samples, makes it difficult to understand the origin of elasticity in drawn or extruded samples. Loos et al.[25] analyzing melt-spun sPP single filament fibers associated elasticity to a rubberlike behavior related to low crystallinity and small micellar crystals in the fiber, acting as physical cross-links in the amorphous matrix.

* Corresponding author: E-mail: vvittoria@.unisa.it.

10.1021/ma011825b CCC: $22.00
Published on Web 04/16/2002

Auriemma et al.[26] analyzing sPP fibers cold drawn at room temperature concluded that while the driving force which induces the recovery of the initial dimensions in common elastomers upon release of the stress is mainly entropic, in the case of sPP it is basically linked to the enthalpy gain achieved when the sample is relaxed, which involves a crystal−crystal phase transition from the metastable form III to the more stable helical modification (form II). Guadagno et al.,[5, 27−28] drawing at room-temperature samples either in the helical or in the trans-planar form, found that, despite a different and complex structural organization of the elastic fibers, their behavior was qualitatively very similar. Elasticity was suggested to be closely associated with—even though not necessarily dependent on—a conformational transition from helical to trans-planar of molecules both within and connecting different crystalline blocks along the fiber direction. The amorphous phase, present in a relevant fraction and plausibly at least partially oriented, was thought to be very likely to play an important role in the elastic behavior. The difficulty understanding the origin of the elastic behavior comes, at least in part, from the superposition in the X-ray patterns of helical and trans-planar reflections.[27,28]

We now succeeded in preparing a fiber characterized by a much simpler structural organization yet showing elastic behavior, and here we present the results. It was obtained by quenching the sPP melt in an ice−water bath, directly drawing it at 0 °C up to a draw ratio of 6 and leaving the fiber under tension for 10 days in the cold bath. In this way, we obtained a very simple and stable structural organization, avoiding the formation of the helical crystalline phase when the sample was brought to room temperature and relaxed. The investigation of the structure and of the elastic behavior of this sample allows us to put the understanding of the elasticity of oriented sPP on firmer bases. In addition it helps to develop more reliable models of the structural organization in the previously hypothesized trans-planar mesophase.[22]

Experimental Section

Syndiotactic polypropylene was synthesized according to a previously reported procedure[4] by Prof. P. Longo at the University of Salerno. It showed respectively $M_w = 84\,000$ and $M_n = 40\,000$.

The polymer was analyzed by ^{13}C NMR spectroscopy at 120 °C on an AM 250 Bruker spectrometer operating in the FT mode at 62.89 MHz, by dissolving 30 mg of sample in 0.5 mL of $C_2D_2Cl_4$. Hexamethyldisiloxane was used as internal chemical shift reference. The polymer showed 91% syndiotactic pentads.

Polymer powders were molded in a hot press, at 150 °C, forming a film 0.2 mm thick, and rapidly quenched in an ice−water bath (sample A). Sample A was directly drawn in the cold bath at 0 °C up to a draw ratio of 6, defined as $\lambda = l/l_0$, where l and l_0 are the final and the initial length, respectively. The drawn sample was left fixed in the bath for 10 days (sample 6A). Then it was extracted and analyzed by X-rays and FTIR. After 24 h, tension was released, and the relaxed fiber (sample 6AR) was again analyzed. Upon releasing at room temperature, the sample underwent a large shrinkage, going from $\lambda = 6$ to $\lambda = 4.5$.

Fiber diffraction spectra were recorded under vacuum by means of a cylindrical camera with a radius of 57.3 mm and the X-ray beam direction perpendicular to the fiber axis (Ni-filtered Cu Kα radiation). The Fujifilm BAS-1800 imaging plate system was used to record the diffraction patterns.

Differential scanning calorimetry (DSC) was carried out over the temperature range −100 to +250 °C using a Mettler TA 4000 thermoanalyzer equipped with DSC 30 cell purged with nitrogen and chilled with liquid nitrogen. Heating rates were typically 10 °C/min.

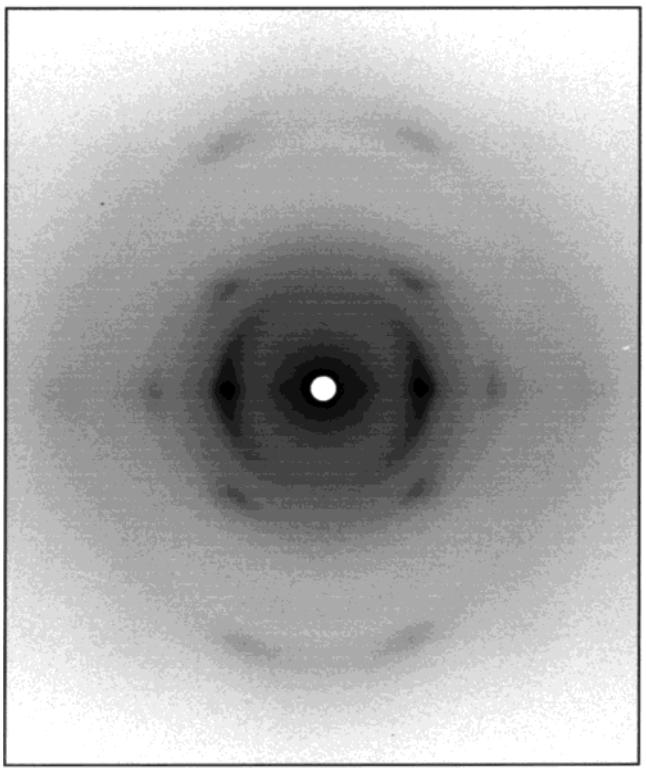

Figure 1. X-ray diffraction pattern of the fixed fiber (sample 6A) with draw ratio $\lambda = 6$.

Infrared spectra were obtained at room temperature using a Bruker IFS66 FTIR spectrophotometer with a resolution of 4 cm^{-1} (32 scans collected). The absorbances of the conformational bands were normalized with the absorbance of the band at 1153 cm^{-1}. Since the investigated bands overlap with other vibrational modes, they were decomposed in their different components, using a complex fitting in which a Lorentzian and a Gaussian contribution were considered in the following form:

$$f(x) = (1 - L)H \exp - \left[\left(\frac{x - x_0}{w}\right)^2 (4 \ln 2)\right] + L \frac{H}{4\left(\frac{x - x_0}{w}\right)^2 + 1}$$

where x_0 is the peak position, H is the height, w is the width at half-height and L is the Lorentzian component.

The elastic behavior of the unhooked fiber was analyzed through hysteresis cycles,[29] performed using an INSTRON 4301 dynamometric apparatus, at room temperature. The deformation rate was 10 mm/min, and the initial length of the sample was 4 mm. The elastic modulus was obtained with the same apparatus for different draw ratios, between $\lambda = 4.5$ and $\lambda = 6.0$, starting from the defined deformation λ, and giving to the sample a further deformation of 0.1%.

Results

X-ray Analysis. In Figure 1, we present the X-ray pattern of sample 6A stretched to a draw ratio of 6 and still under tension. The pattern shows that in essence the crystalline trans-planar form III of sPP was obtained.[10] On the equator we observe the 020 and 110 reflections reported by Chatani and also the weak 130 reflection of the same structure. On the first layer, the 021 and the weaker 111 reflections of the trans-planar form, corresponding to an identity period of 5.05 Å, are

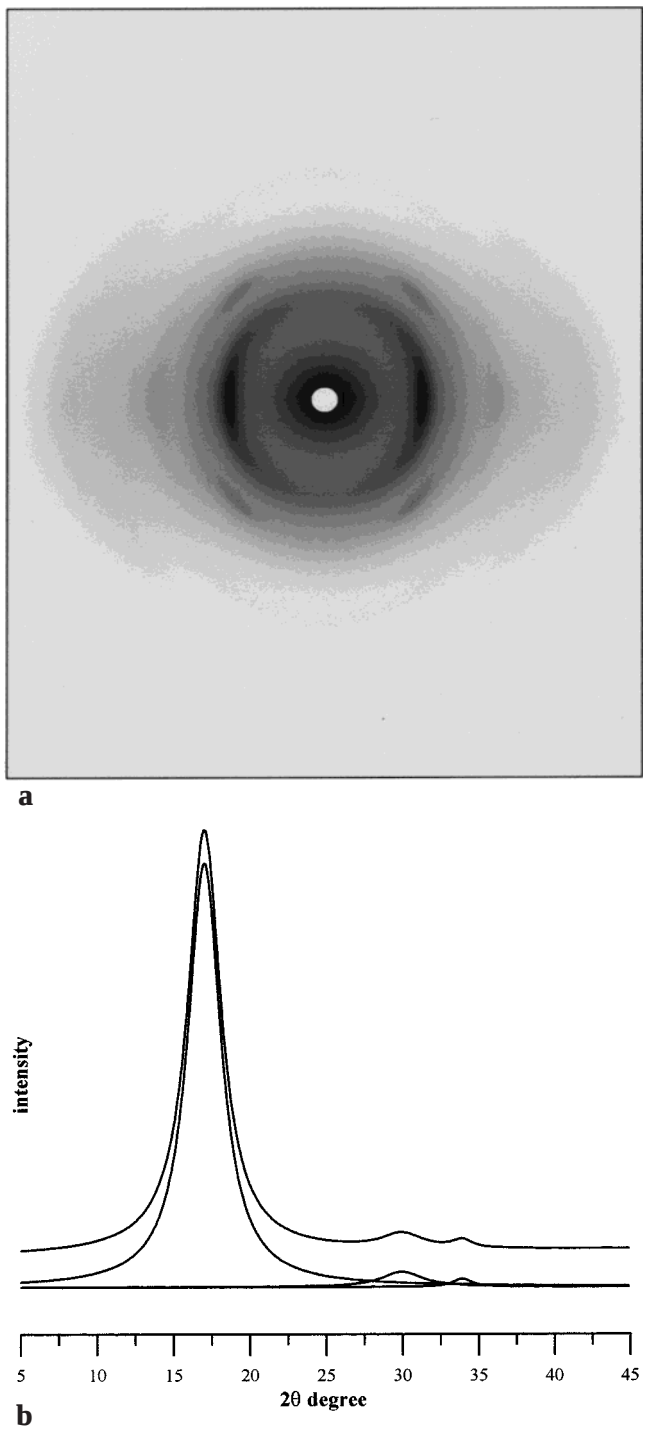

Figure 2. X-ray diffraction pattern of the relaxed fiber (sample 6AR) (a) and equatorial scan of the X-ray intensity (b) with the peaks obtained by deconvolution, using Lorentian fitting.

apparent. No evidence at all of reflections due to helical forms are observed.

Upon releasing tension the fiber underwent a 25% shrinkage, contracting from $\lambda = 6$ to $\lambda = 4.5$. The X-ray pattern of the unhooked fiber, shown in Figure 2a, is clearly different from that in Figure 1, while being fully compatible with those of the unoriented systems interpreted either as form III[21] or as a disordered transplanar mesophase.[22] The sample is thus the first oriented system of this kind to be described, although it is less oriented than the fully stretched fiber. No helical reflections are again observed while there is a clear decrease in crystallinity, the broad amorphous halo at 2ϑ about 17−18° being much more prominent and isotropic. Three reflections are apparent on the equator, namely a very intense one at $2\vartheta = 17.0°$ ($d = 5.21$ Å) a weak reflection and a very weak one respectively at $2\vartheta = 29.7°$ ($d = 3.01$ Å) and at $2\vartheta = 34.4°$ ($d = 2.61$ Å). The equatorial maxima can be indexed as 100, 110, and 200 due to a pseudohexagonal lattice with $a = 6.02$ Å. Such a one-chain unit cell is the most obvious first hypothesis for a mesomorphic phase. The analysis of the intensity on the equator is on the other hand inconsistent with form III (see Figure 1) which has its two strong equatorial maxima at $2\vartheta = 15.9$ and 18.8° (020 and 110) with a third weaker maximum at $2\vartheta = 29.5°$ (130). Considering the scan of the X-ray pattern intensity of the relaxed fiber, reported in Figure 2b the observed peak at $2\vartheta = 17.0°$ has a fwhm of ca. 2.5° and can hardly be considered the result of two peaks of comparable intensity ca. 3.0° apart, unless substantial perturbations of the lattice are assumed.

On the first layer, we observe only one reflection at $2\vartheta = 23.7°$ which cannot be indexed with the pseudohexagonal unit cell, since, excluding the 001, the lowest angle first layer reflection would be at 24.5°. A possible explanation could be that the mesophase has no first layer reflection and the maximum observed at $2\vartheta = 23.7°$ is due to a form III impurity, since this phase has indeed a strong 021 reflection in this position. This explanation is however unlikely as none of the other strong form III reflections on the equator or on the first layer are unequivocally observed. Therefore, at most minor proportions of form III may be present. Furthermore, the full width at half-maximum (fwhm) and the azimuthal spread of the first layer reflection and of the equatorial maxima are comparable, suggesting that they are due to the same phase.

A more plausible interpretation of the diffraction pattern results adopting an orthohexagonal lattice with $a = 6.02$, $b = 10.42$, and $c = 5.05$ Å. (i.e., with a volume twice the one of the hexagonal cell). Assuming two chains in the unit cell, a density value of 0.88 g cm^{-3} results, i.e., 7% smaller than that of form III but 3% larger than the amorphous phase. The equatorial reflections are now indexed as 110 and 020 at $2\vartheta = 17.0°$, 200 and 130 at $2\vartheta = 29.7°$, and 220 and 040 at $2\vartheta = 34.4°$. The first layer maximum centered at $2\vartheta = 23.7°$ can be interpreted, considering its fwhm of about 2.5°, as the result of the contributions of reflections 101 and 111 at $2\vartheta = 23.0°$ and 24.5, respectively. This interpretation of the pattern implies a mesophase model with a centered projection packing, somewhat reminiscent of form III. Diffuse scattering along the first layer line, except for one relatively sharp maximum, indicates limited order along the chain direction and scarce, but nonnegligible, intermolecular correlation along the axial direction. The diffuse features of the second layer line meridional intensity in tilted patterns of the mesophase, as compared to the corresponding form III patterns, suggest some conformational disorder.

Summarizing, on releasing tension, the crystalline form III transformed into an oriented mesomorphic form characterized by the chains in trans-planar conformation and describable, at least to a first approximation, with an orthohexagonal model. As can be observed in the equatorial scan of the X-ray pattern intensity, reported in Figure 2b, the peak centered at $2\vartheta = 17.0°$

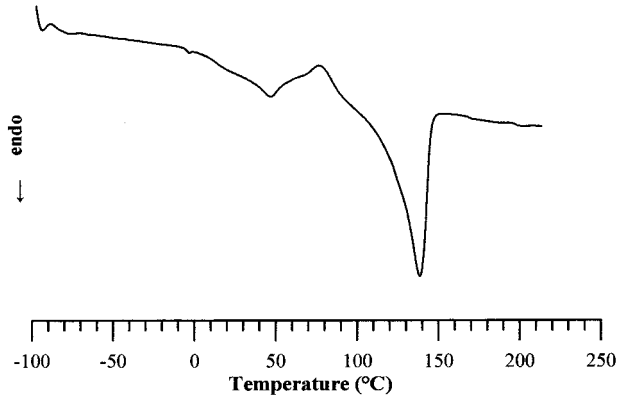

Figure 3. Differential scanning calorimeter curve of the relaxed fiber 6AR.

has a fwhm of ca. 2.5° corresponding to a domain size of about 30 Å as estimated using the Scherrer equation. This gives an indication of the degree of order shown by these ordered domains in a direction orthogonal to the chain axis.

Differential Scanning Calorimetry (DSC). In Figure 3, we report the thermogram of the relaxed fiber 6AR. At low-temperature we observe a pronounced deflection of the baseline in the −5 to +15 °C range, due to the glass transition. An endothermic peak is evident in the curve centered at 46 °C and extending to 65 °C. In the case of nonoriented sPP samples, this endothermic peak was associated with the melting or disordering of a mesophase formed when the samples were quenched from the melt and/or aged at room temperature.[4,30,31] In the present case, we can associate the small endothermic peak to the melting of the mesophase formed upon relaxing the fiber from the metastable trans-planar crystalline form, as shown by X-ray analysis. The disordering of the trans-planar mesophase is immediately followed by a large exothermal peak, centered at 77 °C. It is known that the trans-planar form transforms into the helical crystalline form at temperatures higher than 60 °C,[16−19] and therefore the observed exothermal peak, following the disordering of the mesophase, can be associated with the crystallization. The crystalline helical phase, formed during the heating scan, shows the usual melting peak centered at 138 °C.

The pronounced baseline deflections due to the glass transition and the large exotherm, following the disordering of the mesophase, indicate that the relaxed fiber, besides having a substantial trans-planar mesophase component, is largely amorphous. This result was already found in melt-spun fibers.[25] In addition, it is worth recalling that, in all the investigated cases, the proportion of unoriented trans-planar mesophase formed at 0 °C does not reach values higher than 25−30%, even after very long times of permanence in the cold bath.[21−24]

Infrared Analysis. In Figure 4 we show the FTIR spectra of samples 6A (a) and 6AR (b). In the fixed fiber, the helical bands[32,33] at 810 and 1005 cm^{-1} are hardly distinguishable, and only the band at 977 cm^{-1} appears as a shoulder of the 963 cm^{-1} band. This result confirms the X-ray results with respect to the crystalline phase and in addition shows that chains in helical conformation are not present even in the amorphous component of the sample.

In the FTIR spectrum of the relaxed fiber 6AR (Figure 4b) a very small increase of the helical band at 977 cm^{-1} is clearly observable. Repeated cycles of stretching and releasing the fiber between $\lambda = 6.0$ and $\lambda = 4.5$, which is in the elastic range, demonstrate that the helical band at 977 cm^{-1} decreases and increases accordingly. The spectra of the fiber stretched for the second time and of the fiber released again are shown in Figure 4, parts c and d, respectively..

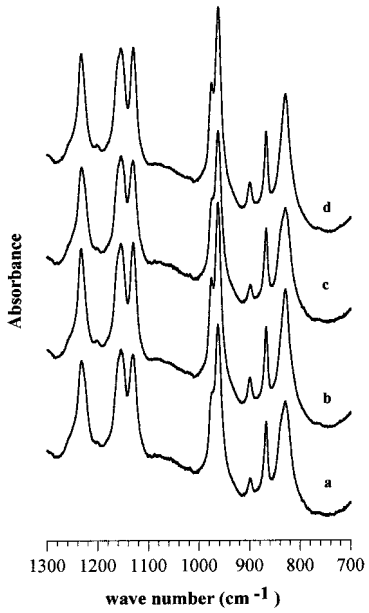

Figure 4. FTIR spectra in absorbance (1300−700 cm^{-1}) of the fixed fiber 6A (a), the relaxed fiber (b), the fiber again stretched (c), and the fiber again released (d).

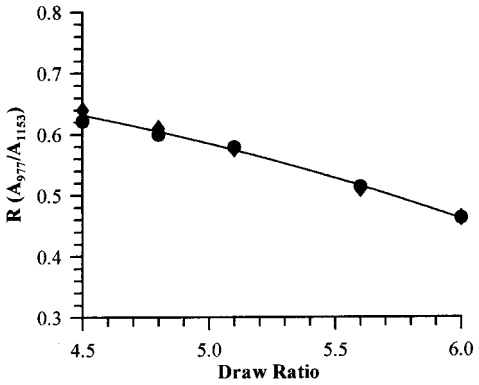

Figure 5. Ratio R reported as a function of λ between $\lambda = 4.5$ (relaxed fiber) and $\lambda = 6$ (fixed fiber), during stretching (◆) and releasing (●) tension.

Since the fiber thickness changes on stretching and releasing, due to the strong shrinkage on unhooking, we followed the quantitative behavior of the helical 977 cm^{-1} band normalizing the absorbance of this band with the absorbance of the 1153 cm^{-1} band, which is independent of the conformation[34] obtaining the ratio:

$$R = \text{absorbance}(977\ cm^{-1})/\text{absorbance}(1153\ cm^{-1})$$

The band at 1153 cm^{-1}, which overlaps with other vibrational modes, was decomposed into the different components, as shown in the Experimental Section. Also the absorbance of the helical band at 977 cm^{-1}, overlapping with the trans-planar band at 963 cm^{-1}, was obtained by a similar decomposition procedure.

In Figure 5, we show the behavior, both in the stretching process and in the releasing process of the fiber, of the ratio R as a function of λ between $\lambda = 4.5$,

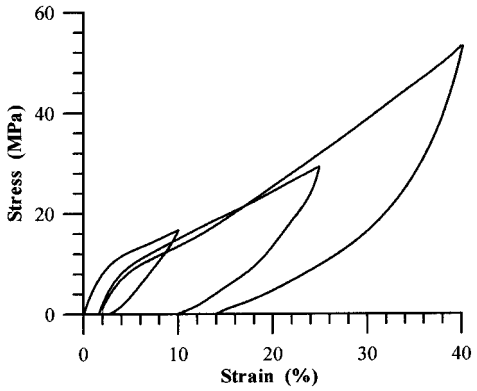

Figure 6. Hysteresis cycles of sample 6AR.

Table 1. Mechanical Parameters Derived from the Hysteresis Cycles.

hysteresis cycle	cycle 1	cycle 2	cycle 3
energy losses (%)	53	62	60
tension set (%)	3	10	14

i.e., for the unhooked fiber (sample 6AR), and $\lambda = 6.0$ (the fixed fiber, sample 6A). We observe that there is a continuous although modest increase of the helical band upon releasing the tension and a corresponding decrease upon stretching the sample again. Since the experimental points fit the same curve during stretching and releasing the tension, we deduce that the formation of the helical chains is reversible in the elastic range. Moreover, considering that in the X-ray pattern of sample 6AR (Figure 2) there is no evidence of any helical crystalline reflection, we can infer that, on releasing the tension, some chain fragments adopt the helical conformation, but they are not located in a positions suitable for crystallization in the helical modifications. During the second stretching these chains reversibly decrease, and it is likely that they adopt trans-planar conformations as a part of an ordering process leading to substantial crystallization into form III and to increased degrees of orientation. These tie chains are possibly incorporated into the crystalline form III or remain as bridges between the crystals, but in any case they return to the helical conformation when the metastable crystalline form III is transformed back into the mesophase.

Elastic Behavior. In the range between $\lambda = 6.0$ and $\lambda = 4.5$, the fiber shows elastic behavior. In Figure 6, we report hysteresis cycles for our samples which were deformed at strain values progressively increasing, step by step, from the relaxed length ($\lambda = 4.5$) to the highest previously reached length ($\lambda = 6.0$), recording the stress while increasing and decreasing the strain. The area of each hysteresis curve, reported in Table 1, represents the energy dissipated in the cycle which increases on increasing the strain. The permanent set, that is the residual deformation after each cycle, reported in Table 1, is very low, reaching 14% for the maximum strain, and it is almost eliminated after 2 h of rest.

Therefore, sample 6AR has remarkable elastic properties, with a modulus some orders of magnitude higher than those for a conventional elastomeric material. Moreover the elastic modulus strongly increases on deforming the fiber from the relaxed state (sample 6AR) to the stretched state (sample 6A). This behavior, completely different from a conventional elastomer, is shown in Figure 7 where the elastic modulus is reported as a function of the deformation. We can observe a more than linear increase of elastic modulus on increasing the deformation: it is 340 MPa for the relaxed fiber and reaches the very high value of 1.12 GPa for the fixed fiber. This very large increase of the elastic modulus on increasing the deformation is consistent with a mechanism in which the amorphous component of the fiber is progressively more and more constrained and deformed from it equilibrium state. The observed effects can be explained by considering that in the stretching process the trans-planar mesophase and some amorphous materials are largely transformed into the crystalline form III. Moreover some chains, present in the relaxed fiber in helical conformation, progressively disappear during the stretching. Strain-induced crystallization and the increasingly anisotropic conformation of molecules in the amorphous phase may determine the large value of the elastic modulus and its increase upon further deformation. In this picture, it is assumed that, upon further elongation, increasing numbers of intercrystalline tie molecules achieve a highly extended, entangled, and strained state, which cannot sustain further deformation.

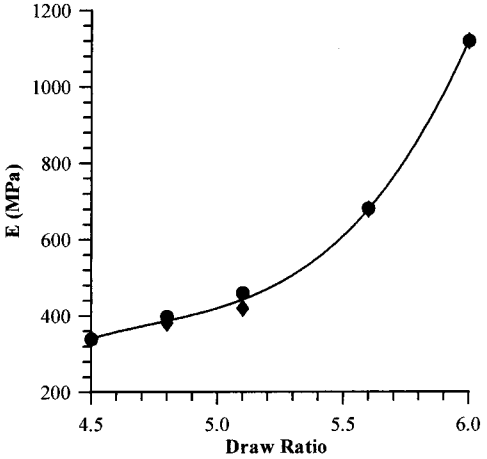

Figure 7. Elastic modulus reported as a function of deformation λ between $\lambda = 4.5$ (relaxed fiber) and $\lambda = 6$ (fixed fiber), during stretching (◆) and releasing (●) tension.

Discussion

The behavior of oriented sPP is reminiscent of the so-called "hard elastic fibers" of isotactic polypropylene (iPP) investigated some years ago.[35,36] In that case, elasticity was correlated to the row-nucleated morphology, due to particular processing conditions. High elastic modulus, high elastic recovery, and large extensions were attributed to a combination of factors, and models were developed to take into account the nonconventional elastic response.

In the case of syndiotactic polypropylene no unusual processing conditions are needed to obtain elastic fibers characterized by high elastic modulus and high elastic recovery. Previous investigations have demonstrated that melt extrusion[25] as well as drawing of different polymorphs at room temperature[5,27,28] produce elastic fibers when tension is released after drawing. In all investigated cases, the fully elongated fibers have high contents of crystalline form III. On the other hand, the relaxed fibers can show different X-ray patterns, which are due to helical or trans-planar sPP modifications or mixtures thereof.

The fact that when the fully elongated fibers are unhooked, a large shrinkage occurs and some or all of the form III crystallinity is lost relates to the instability of this sPP modification. On the other hand, we note that all sPP fibers must contain a nonnegligible amorphous fraction, possibly oriented, which will form the mechanically weaker domains, bound to play a major role in the elasticity of sPP. It is also important to notice also that all the relaxed fibers show a very similar elastic behavior, despite the different structures shown by X-ray diffraction.[5,27−28]

The above observations point to a mechanism underlying the elastic behavior of sPP, in which strain induced-crystallization into an intrinsically unstable crystalline form has a key role. The fact that sPP elasticity is largely independent of the crystalline phase in the unhooked fiber, also seems consistent with a conventional rubberlike behavior, dependent only on the amorphous fraction.[37] However, some key facts indicate that standard explanations are insufficient: (i) the elastic behavior occurs at temperatures much lower than the melting point of the unstrained system; (ii) the elastic modulus is orders of magnitude higher; (iii) the elastic behavior is shown only by material that, even when relaxed, remains largely oriented and in some form highly ordered. Furthermore, the hysteretic behavior and the thermomechanical measurements in progress in our laboratory[38] indicate that, at least in some instances, there is an enthalpic component in the elasticity of sPP.

The sample analyzed in this paper, directly drawn from the melt at 0 °C and left in the cold bath for many days, shows a relatively simple structural organization and can help clarify the origin and the peculiar features of elasticity in sPP. When fixed, the sample is in the crystalline trans-planar form III, whereas when relaxed it transforms from the crystalline form III into a less oriented mesophase, still showing the chains in trans-planar conformation. This behavior is reproduced in successive cycles. From X-ray diffraction no evidence of helical reflections appears both in the fixed and in the relaxed fiber. IR measurements show that in the elastic range, upon relaxation some helical segments are reversibly formed, which however reside in amorphous domains. When the fiber is repeatedly released and stretched, the helical bands increase and decrease accordingly, implying that strain reversibly involves also these molecules. It indeed is somewhat surprising, that in successive room-temperature cycles the fiber returns, upon relaxation to the mesomorphic phase, which is metastable, no less than form III.

The above behavior is consistent with reports that successive relaxation cycles of sPP elastic fibers bring approximately to the same original phase composition and not necessarily to the more stable crystalline phase. It suggests a highly constrained system where modifications occur at a local level, and the fiber as a whole is very far from a global equilibrium condition.

Considering the overall picture, it is clear that many factors may contribute to the elastic behavior of sPP. When the elastic fiber—in which, along with some oriented amorphous phase, the helical, the trans-planar crystalline, or the mesophase may be present—is progressively elongated in the elastic range, it may well undergo a process of local melting to an oriented amorphous very rapidly followed by strain induced crystallization forming the trans-planar modification III. Direct transitions from the mesophase to form III, not involving the amorphous, can also be envisaged: indeed we can speculate that the mesophase could represent the intermediate state in cases where strain induced transformations from helical crystal forms to modification III occur. Direct transformations between helical and trans-planar crystals not involving locally disordered amorphous or mesomorphic states appear unlikely in such a complex multiphase system. It is of course impossible to rule them out completely.

Not only do the mesomorphic chains converge into the oriented form III crystals, but also some of the original, more or less oriented, amorphous chains are involved in the deformation process consistent with views closer to a classical elasticity mechanism. Such chains, acting as bridges between the crystals, are either highly entangled and constrained or they adopt relatively ordered, extended conformations, in any case far from the equilibrium value. All the newly form III crystals are relatively small and highly strained: therefore their melting points are greatly depressed. When tension is released, both the noncrystalline domains and the form III crystals are subjected to entropic retractive forces. Depending on local conformations and strains also enthalpic contributions can be envisaged. These bring the sample back to a situation which is very close to the original non strained state and maintain the orientation, although less than before the relaxation. The conformation of the highly extended and constrained molecules in the amorphous domains must indeed have a key role in the whole process. Such "knotted" noncrystallne chains appear to be largely responsible for ultimate elastic behavior of sPP.

In depth thermomechanical and structural investigation are in progress to resolve experimentally the entropic and enthalpic contributions to the elastic behavior of sPP.

Acknowledgment. This work was supported by Ministero dell'Università e della Ricerca Scientifica e Tecnologica (PRIN 2000 titled "Selective polymerization: coordination catalysts and control of physical properties of the resulting polymers" and PRIN 1999 titled "Polymer interphases and crystallization" for S.V.M.). Encouraging discussions with professor Giuseppe Allegra are gratefully acknowledged.

References and Notes

(1) Uehara, H.; Yamazaki, Y.; Kanamoto, T. *Polymer* **1996**, *37*, 57.
(2) Loos, J.; Huckert, A.; Petermann, J. *Colloid Polym. Sci.* **1996**, *274*, 1006.
(3) Loos, J.; Petermann, J.; Waldofner, A. *Colloid Polym. Sci.* **1997**, 10888.
(4) Guadagno, L.; Fontanella, C.; Vittoria, V.; Longo, P. *J. Polym. Sci., Part B* **1999**, *37*, 173.
(5) D'Aniello, C.; Guadagno, L.; Naddeo, C.; Vittoria, V. *Macromol. Rapid Commun.* **2001**, *22*, 104.
(6) Lotz, B.; Lovinger, A. J.; Cais, R. E. *Macromolecules* **1988**, *21*, 2375.
(7) Lovinger A. J.; Lotz, B.; Cais, R. E. *Polymer* **1990**, *31*, 2253.
(8) Lovinger, A. J.; Davis D. D.; Lotz, B. *Macromolecules* **1991**, *24*, 552.
(9) Lovinger A. J.; Lotz, B.; Davis D. D.; Padden, F. J. *Macromolecules* **1993,** *26*, 3494.
(10) Chatani, Y.; Maruyama, H.; Noguchi, K.; Asanuma, T.; Shiomura, T. *J Polym. Sci. Part C* **1990**, *28*, 393.
(11) Chatani, Y.; Maruyama, H.; Asanuma, T.; Shiomura T. J. *J. Polym. Sci. Polym. Phys. Ed.* **1991,** *29*, 1649.
(12) De Rosa, C.; Corradini, P. *Macromolecules* **1993**, *26*, 5711.

(13) Auriemma, F.; Lewis R. H.; Spiess, H. W.; De Rosa, C. *Macromol. Chem. Phys.* **1995**, *196*, 4011.
(14) De Rosa, C.; Auriemma, F.; Corradini, P. *Macromol. Chem.* **1996**, *29*, 7452.
(15) De Rosa, C.; Auriemma, F.; Vinti, V. *Macromolecules* **1997,** *30***,** 4137.
(16) De Rosa, C.; Auriemma, F.; Vinti, V. *Macromolecules* **1998,** *31***,** 9253.
(17) Lacks D. J. *Macromolecules* **1996,** *29***,** 1849.
(18) Palmo, K.; Krimm, S. *Macromolecules* **1996**, *29***,** 8549.
(19) Uehara, H.; Yamazaki, Y.; Kanamoto, T. *Polymer* **1996**, *37*, 57.
(20) Loos, J.; Buhk, M.; Petermann, J.; Zoumis, K.; Kaminsky, W. *Polymer* **1996**, *37*, 387.
(21) Nakaoki, T.; Ohira, Y.; Hayashi, H.; Horii, F. *Macromolecules* **1998**, *31*, 2705.
(22) Vittoria, V.; Guadagno, L.; Comotti, A.; Simonutti, R.; Auriemma, F.; De Rosa, C. *Macromolecules* **2000**, *33*, 6200.
(23) Nakaoki, T.; Yamanaka, T.; Ohira, Y.; Horii, F. *Macromolecules* **2000**, *33***,** 2718.
(24) Nakaoki, T.; Yamanaka, T.; Horii, F. *Polymer* **2001**, *42***,** 4555.
(25) Loos, J.; Shimanski, T. *Polym. Eng. Sci.* **2000**, *40*, 567.
(26) Auriemma, F.; Ruiz de Ballestreros, O.; De Rosa, C. *Macromolecules* **2001**, *34*, 4485.
(27) Guadagno, L.; D'Aniello, C.; Naddeo, C.; Vittoria, V. *Macromolecules* **2001**, *34*, 2512.
(28) Guadagno, L.; D'Aniello, C.; Naddeo, C.; Vittoria, V. *Macromolecules* **2000**, *33*, 6023.
(29) Treloar L. R. G.; *The Physics of Rubber Elasticity*; Clarendon Press: Oxford, England, 1973.
(30) Guadagno, L.; D'Arienzo, L.; Vittoria, V.; Longo, P.; Romano, G. *J. Macromol. Sci. Phys.* **2000**, *B39*, 425.
(31) Schwartz, J.; Stranz, M.; Bonnet, M.; Petermann, J. *Colloid Polym. Sci.* **2001**, *506*, 279.
(32) Natta, G.; Corradini, P.; Ganis, P. *Makromol. Chem.* **1960**, *39*, 238.
(33) Natta, G.; Pasquon, I.; Corradini, P.; Peraldo, M.; Pegoraro, M.; Zambelli A. *Rend. Acc. Naz. Lincei* **1960**, *28*, 539.
(34) Guadagno, L.; D'Arienzo, L.; Vittoria, V. *Macromol. Chem. Phys.* **2000** *201*, 246.
(35) Cannon S. L.; McKenna G. B.; Statton W. O. *J. Polym. Sci., Macromol. Rev.* **1976**, *11*, 209.
(36) Noether H. D.; Whitney, W. *Kolloid Z. Z. Polym.* **1973**, *251*, 991.
(37) Allegra, G.; Bruzzone, M. *Macromolecules* **1983**, *16*, 1167.
(38) Guadagno, L.; D'Aniello, C.; Vittoria, V.; Naddeo, C.; Romano, G. Submitted for publication.

MA011825B